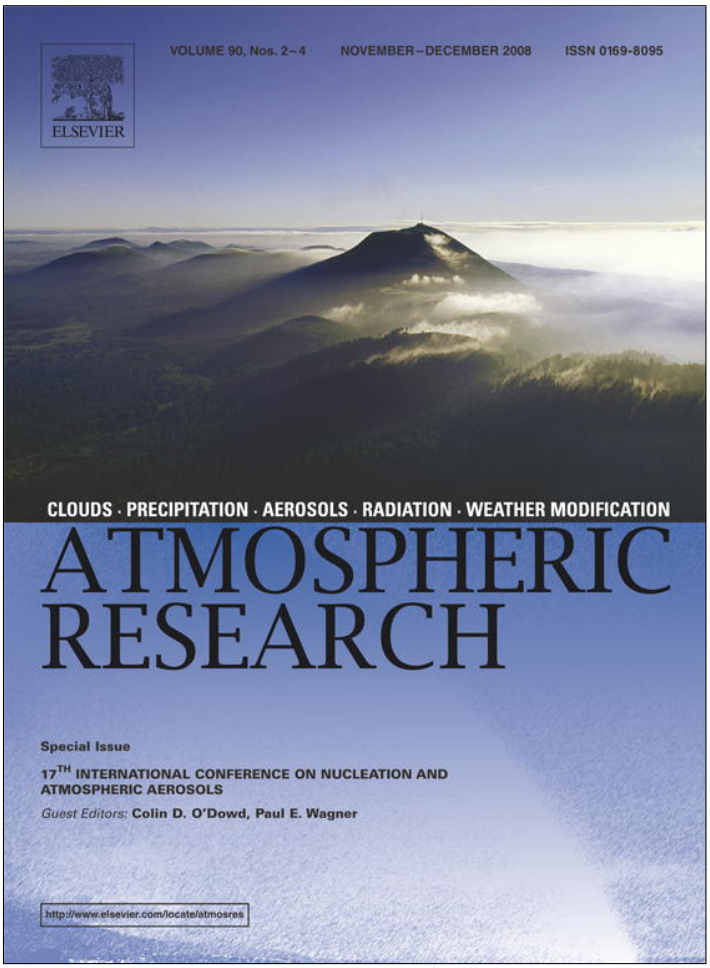

Atmospheric Research 90 (2008) 326–337

Contents lists available at ScienceDirect

Atmospheric Research

journal homepage: www.elsevier.com/locate/atmos

Effect of soot on immersion freezing of water and possible atmospheric implications

O. Popovicheva [a,*], E. Kireeva [a], N. Persiantseva [a], T. Khokhlova [b], N. Shonija [b], V. Tishkova [c], B. Demirdjian [c]

[a] Institute of Nuclear Physics, Moscow State University, Moscow, Russia
[b] Chemical Department, Moscow State University, Moscow, Russia
[c] CINaM / UPR CNRS 3118, Marseille, France associated to Aix-Marseille University

ARTICLE INFO

Article history:
Received 1 October 2007
Received in revised form 30 July 2008
Accepted 12 August 2008

Keywords:
Ice nucleation
Soot
Immersion freezing
Wetting
Hydration

ABSTRACT

More than 3000 water droplets with soot particles immersed were monitored individually to identify the effect of heterogeneous freezing and establish the link between soot properties and freezing efficiency. A set of soot samples from many combustion sources, including an aircraft engine combustor were examined. The list of key soot properties affecting freezing were determined. It appears that soot effectiveness in causing the droplets to freeze mainly depends on the soot behaviour in water defined by the mass density of soot agglomerates, size and wetting. When large mass particles were homogeneously distributed through droplets and were stable to sedimentation effects median freezing temperatures of such droplets were significantly warmer than pure water droplets. The long-term presence of large soot agglomerates in water leads to an increase in the freezing efficiency over time because of the slow kinetics of wetting. Small sizes of soot agglomerates stimulate aggregative instability in droplets with large soot mass which decreases the total soot surface area and the freezing temperature. The highest freezing efficiency is found for homogeneously distributed soot agglomerates of high porosity. A gradual increase of the freezing temperature in correspondence with number density of active oxygen-containing sites is observed for soots having surfaces of low or intermediate polarity. However, highly soluble surface compounds, such as sulfates, may be easily dissolved in water leading to a decrease in the potential freezing efficiency. This was the case found for aircraft engine combustor generated soot. Therefore relatively hydrophobic soot with a significant number of oxygen-containing functional groups but not covered totally by hydrophilic sites and soluble compounds is proposed to act as the most efficient immersion freezing nuclei in the atmospheric cloud droplets.

1. Introduction

Field measurements of deduced threshold relative humidity conditions for cirrus cloud formation at a Northern Hemisphere location suggest the possibility that pollution plays a role in controlling cirrus formation (Haag et al., 2003). High concentrations of nonvolatile particles found within contrail and cirrus crystals suggest the possible role of black carbon (soot) as ice nuclei in these clouds (Petzold et al., 1998; Kuhn et al., 1998). Carbonaceous particles have been inferred as the core species within ice nuclei processed from aircraft exhaust plumes, ranging from 10 to 60% of all the ice nuclei at times (Chen et al., 1998), although similar numbers of carbonaceous particles were found as IN in the ambient atmosphere and no IN enhancement in exhaust plumes was detected compared to the background air. Other studies report carbonaceous particles as IN and ice cloud residuals, some specifically identified as soot, ranging from 2 to 60% (DeMott et al., 2003; Rogers et al., 2001; Twohy and Poellot,

* Corresponding author.
E-mail address: polga@mics.msu.su (O. Popovicheva).

0169-8095/$ – see front matter © 2008 Elsevier B.V. All rights reserved.
doi:10.1016/j.atmosres.2008.08.004

2005). Other studies suggest that soot aerosols from evaporated contrails may affect the microphysical properties of natural cirrus clouds (Strom and Ohlsson, 1998). The optical observations of an internal mixture of ice-BC aerosols in the aircraft plume (Kuhn et al., 1998) may confirm theoretical model predictions of the contrail formation (Kärcher et al., 1996) assuming that exhaust soot particles may serve as IN.

Homogeneous nucleation of ice is important mainly in the upper troposphere while at the lower altitudes ice formation necessarily occurs by heterogeneous nucleation at higher temperatures. However, the mechanism that could lead to heterogeneous ice nucleation by soot particles at the cirrus level and in the lower-tropospheric clouds is not clear. Laboratory studies (Dymaska et al., 2006) simulate the direct deposition ice nucleation on certain soot. Numerical simulations (DeMott et al., 1997; Jensen and Toon, 1997) focus on immersion freezing nucleation because of the low likelihood of finding completely insoluble particles available for direct ice deposition nucleation. The lack of observation and laboratory data has lead the investigators (Gierens,2003; Lohmann et al., 2004) to evaluate the effectiveness of heterogeneous freezing versus homogeneous freezing hypothetically assuming that soot particles act as immersion freezing nuclei at an ice supersaturation of 30%. They conduct a scenario with hypothetically assumed heterogeneous freezing ability of soot particles where the specific soot physico-chemical properties are not considered.

However, soot particles emitted into atmosphere from a great variety of combustion sources have a wide range of a natural variability with respect to physico-chemical properties, including the composition and hygroscopicity. Jensen and Toon (1997) have examined the ice nucleation activity by variation of the contact angle as a parameter for upper tropospheric soot particles. They demonstrated that even with sufficient concentration of relatively poor heterogeneous nuclei the freezing temperature of cirrus clouds could be substantially increased. Moreover, the importance of the heterogeneous freezing compared to the homogeneous freezing nucleation process depends greatly on the particle size and the mass percent in the droplet (DeMott et al., 1997). The presence of insoluble particulates at sizes greater than 0.5 μm within just a few percent of cloud condensation nuclei (CCN) population lowers ice crystal concentration by an order of magnitude in comparison with smaller size particles of 0.08 μm. Therefore, the effect of large soot agglomerates immersed into droplets should be considered equally with effect of the primary particles.

Unfortunately, sparse documentation exists on the properties of atmospheric soot particles measured at contrail and cirrus levels. The situation is complicated by a limit of possibilities for in-situ exhaust measurement of soot characteristics such as wetting, water uptake, and surface chemistry. For nucleation studies in laboratories commercially available black carbons, spark discharge soot or samples produced by different burners (Dymaska et al., 2006; DeMott, 1990; DeMott et al., 1999; Moehler et al., 2005; Gorbunov et al., 2001) have been used. Diehl and Mitra (1998) found that supercooled water droplets of radius between 170 and 410 μm polluted by kerosene-burner exhausts freeze at significantly warmer temperatures than pure droplets. Laboratory studies of acetylene burner soot activity (DeMott, 1990) demonstrated clouds first formed near −22 °C and then that immersion freezing was observed as polluted clouds droplets with a single soot particle continued to cool down −40 °C. Lack of soot characterization data in these studies and absence of comparative analysis with other kinds of soot limits currently the ability to establish the connection between physico-chemical properties of soot particles and their freezing activity.

To address particle wettability, the classical theory of heterogeneous nucleation uses the macroscopic parameter of the droplet contact angle (Pruppacher and Klett, 1978). This parameter determines the rate of heterogeneous freezing of ice germs originating on the substrate active sites. However, a water contact angle is a macroscopic measure, which cannot reveal the nature and the amount of active sites. Nevertheless, it correlates with the level of soot polarity, which may be obtained by measurements of water uptake from vapor phase (Persiantseva et al., 2004). This laboratory approach allows the classification of soots from hydrophobic to hydrophilic, the identification of the role of active sites and soluble compounds. In view of this approach, it is highly questionable whether the soot surface chemistry (presence of active sites and coverage by soluble compounds) impacts the freezing in the atmosphere.

Additionally, the question of the soot particle distribution over droplet volume should be considered; different locations of soot particles within a water droplet were observed by Demirdjian et al. (2007). This question mostly is valid for a massively polluted situation such as in fire-cloud interaction situation.

This paper is devoted to laboratory studies of the heterogeneous freezing of water droplets induced by immersed soot. A set of well-characterized soot samples from many combustion sources is used for examination. The median freezing temperature of the population of soot seeded water droplets is obtained that demonstrates a clear impact of suspension sedimentation and aggregation stabilities as well as soot wetting, hydrophilicity, and water soluble fraction. The characteristics of soot particles active in the immersion freezing mode are thereby suggested. Analysis of properties of original aircraft engine combustor soot allows some conclusions about soot ice nuclei efficiency of one real atmospheric soot in the atmosphere.

2. Material and methods of characterization

2.1. Set of soot and its characterization

To study a wide range of soot properties and estimate independently the impact of different characteristics a *Set of soots* from different sources is proposed in Table 1. A number of commercial soots, recently popular between researches (DeMott, 1990; Dymaska et al., 2006; Lammel and Novakov, 1995) are chosen, such as *Lamp Black*, *FW2 (Channel Black)*, *Furnace Black* and *Thermal (T-900)* soot of Degussa and Ukhta OPP production. Lamp Black (LB) and Furnace Black (FB) were produced in the furnace flame by burning liquid oil or natural gas, respectively; FW2 soot originated from gaseous hydrocarbons in the channel-type process; Thermal soot was obtained by pyrolysis of natural gas.

Typical soot is composed of primary particles, ranging from 0.01 to 0.1 μm, solidly fused together to form aggregates which vary in size between 0.2 and 0.5 μm (Enrburger-Dolle et al., 1990; Mikhailov et al., 1998; Onischuk et al., 2000;

Table 1
Morphological, wetting and chemical characteristics of *Set of soot*

Type of soot	d, nm	S, m^2/g	ρ_o, ρ_s g/cm^3	Porosity ε	Θ, degree	Volatility, %	O, %	W_{me}, cm^3/g
Lamp Black (LB)	95	22	0.15, 0.09	0.925	32	0.6	0.4	0.05
Furnace Black (FB)	35	100	0.28, 0.11	0.86	28	2.3	4.2	0.73
FW2 (Channel Black)	13	420	0.3, 0.14	0.85	40	7.9	9.9	0.9
Acetylene (AS)	50	86	0.09, 0.08	0.95	47	0.1	0.4	0.18
Thermal (T-900)	246	10	0.26, 0.19	0.87	43–58	0.6	0.7	0.01
Aircraft engine combustor (AEC)	48 [a]	12	0.35	0.825		17	1–12 [b]	0.01
TC1 kerosene flame (TC1)	30–50	87	0.05	0.975	59	1.0	2	0.02
TC1 oxidized soot (TC1-O)	57	49	0.02	0.99	69	4.0	5	0.07
Combustor remote (CRS)	30–50	104	0.04	0.98			12.7	0.02

[a] For main fraction.
[b] For fraction of impurities.

Popovicheva et al., 2003a,b). The aggregates are known to associate with one another forming porous agglomerates which unlike the aggregates are breakable when conventional mechanical mixing is used to disperse the compound components. In powder, the agglomerates may form large clusters, from 0.3 up to 1 mm in size. To clarify and eliminate the impact of such huge clusters we have sifted the soot powders cutting off the agglomerates larger 80 μm. A number mass density of the soot bed is measured by filling a calibrated vessel with the soot powder. It is obtained for original and sifted soots, ρ_o and ρ_s, respectively. The total porosity of the soot bed was defined as $\varepsilon = 1 - \rho/\rho_{BC}$, where ρ_{BC} is the primary BC particles density taken as 2 g/cm^3.

A list of morphological characteristics for the *Set of soots* is presented in Table 1. We have summarized the mean diameter of primary particles, d, for FW2 and LB as reported by the producer. For other soots the size distribution was obtained from around six hundred images of primary particles taken by transmission electron microscopy (TEM) using the phase-contrast imaging method described in Demirdjian et al. (2007). The specific surface area, S, was measured by N_2 thermodesorption method (Popovicheva et al., 2000). To obtain the soot texture parameters volumetric adsorption measurements of N_2 at 77.2 K have been performed with a sorptograph technique (ASAP 2010, Micromeritics Instrument). The volume of mesopores, W_{me}, of the size from 4 to 40 nm was estimated from the classical theory of capillary condensation using the BJH method (Gregg and Sing, 1982). The Dubinin's theory of micropores filling (Dubinin and Stoeckli, 1980) was used to obtain the volume of micropores, $W_{mi.}$, of diameter less than 4 nm. Additionally, to estimate the mesopore volume the limited volume of benzene adsorbed at saturation on soots was obtained at 293 K.

The technique of sessile drop measurements (Schrader, 1975) has been used to determine the contact angle, θ, between water droplets and soot surfaces. This method assumes the preparation of the soot pellet with well-controlled surface by compaction of the soot powder (see for details Persiantseva et al., 2004) so that the contact angle is reproducible within the accuracy of four degrees. The data obtained are presented in Table 1. To measure the ice contact angle, water droplets were cooled to 238 K. No measured differences between water and ice were found within the accuracy of this experiment, so further we will report only one value for θ, assuming that it to be valid for both water and ice germs.

The wetting characteristic of soot is sensitive to chemistry of the surface and its purification (Persiantseva et al., 2004). The more hydrophilic is the surface coverage the more effective is the soot–water droplet interaction (Mikhailov et al., 2001). Being the combustion product of hydrocarbon fuels soot particles consist of elemental carbon, hydrophobic in nature, and organic carbon containing oxygen in the form of volatile compounds. In Table 1 we summarize the total oxygen content of FW2 and LB soots as reported by a manufacturer. For other soots XREDS (X-ray Energy Dispersive Spectroscopy) was used to determine the elemental chemical composition (Demirdjian et al., 2007). To estimate the volatile organic fraction, the soot volatility was obtained by the weighing the soot sample before and after heating at 537 K for 30 min using the method of Ohta and Okita (1984) (see Table 1). However, the higher is the oxygen content in the organic coverage the larger may be the water soluble fraction (WSF); water soluble compounds may be easy dissolved when soot is immersed in water. This is why additionally we determined the WSF of soot after immersion into water, filtration and evaporation (see Table 2). A few images of soot agglomerates in water were taken by optical microscopy.

To have soot samples made mostly from elemental carbon (without volatile organic coverage) *Acetylene soot (AS)* produced by acetylene exposure in an oxygen free atmosphere was chosen (production of Ukhta OPP). Its specific properties are described in Kiselev and Kovaleva (1965) and summarized in Table 1.

2.2. Soots of atmospheric application

In applying results obtained with laboratory soot surrogates from different sources to atmospheric systems, it is not clear how the properties of a given laboratory soot relate to real the atmospheric soot aerosols (Popovicheva et al., 2003a). Thus, our understanding of soot-related processes in the atmosphere is limited. One potentially realistic example of atmospheric soot, *aircraft engine combustor soot* (AEC) was produced by a combustor of a modern gas turbine engine, model D30-KU, operating at cruise combustion conditions (Popovicheva et al., 2004). Comparison of the structure and composition of AEC soot with *TC1 kerosene flame soot*,

Table 2
Water soluble fraction and number density of active sites of *Set of soot*

Soots	LB	FB	FW2	AS	T-900	AEC	TC1	TC1-O	CRS
WSF, wt.%	0.4		1.1	~0	0.5	13.5	0.3	1	5
a_m/nm^2	1.5	4.2	2.5	~0	1.1	42	0.8	18	6.3

produced by burning the same TC1 aviation kerosene in oil lamp, have shown the similarity of TC1 soot particles with one fraction of AEC soot. Those particles are free of impurities like sulphur and iron. We here use these two soots in laboratory freezing studies for the estimation of the possible environmental impact of atmospherically available soot surrogates. The specific properties of AEC and TC1 soots are described in Popovicheva et al. (2004), Demirdjian et al. (2007). New samples were produced for this study, their characteristics are summarized in Table 1. Since oxidation of aviation kerosene during long time storage occurs we distinguish between samples before collected, TC1 soot, and the freshly prepared one using stored fuel, TC1 oxidized (TC1-O).

Finally, to investigate the hypothesis about the role of active sites we studied the previously analyzed sample of *combustor remote soot* (CRS) produced by burning sulfur free gaseous propane/butane fuel in a typical combustor of the aircraft engine (Popovicheva et al., 2003a). Oxygen was accumulated on the surface of CRS soot collected far from the combustor exit due to oxidation by hot gaseous exhaust. Thus the use of this soot offers the opportunity to examine the correlation between the soot hydrophilicity and freezing efficiency.

2.3. Water uptake measurements

To address the hydration properties of soot the amount of water molecules adsorbed on the soot surface as a function of the relative humidity is measured by a gravimetrical method proposed by Kantro et al. (1967). We limit the surface cleaning by drying in air at a water vapor pressure of $2 \cdot 10^{-5}$ Torr. Achievement of the equilibrium uptake is controlled by repeatedly weighing the soot sample. The accuracy of water uptake measurements is 3–5%.

3. Freezing measurements

Laboratory measurements of the droplet population freezing are performed by various methods (see a review of DeMott, 2002). One category of experiments examines the behaviour of small droplets dispersed in air. This approach allows measuring the freezing nucleation rates of small supercooled droplets at cirrus conditions (Stockel et al., 2005; DeMott, 1990). Another category of experiments focus on the behaviour of droplet population supported on cold stages (Pruppacher and Klett, 1978; Hoffer, 1961; Koop et al., 1998; Zuberi et al., 2002). Since the effect of the supported surface is always a concern in such studies, precaution is taken to cover the cell surface with a hydrophobic film to minimize the effects of heterogeneous nucleation (Koop et al., 1998; Zuberi et al., 2002; Seeley and Seidler, 2001). This approach was also chosen in our study because it allows monitoring the droplets individually and seeding them with a controlled amount of soot.

Fig. 1 shows the main equipment part of a cell for droplet freezing and of the controlled atmospheric chamber providing a stable cooling rate. Droplets of a given, controllable size are manufactured from distilled water. They rest on the perfectly polished surface of the Teflon cell. The polish pretreatment yielded a hydrophobic surface with a water contact angle of approximately 120°. The equipment was designed to have the possibility of continually viewing the droplets and the controlling the deformation of the droplets from sphericity.

The droplet temperature is continuously measured by the electrical thermometer (Center 306) having a resistance temperature sensor of the K-type that touches the droplet 10 μm under support. Fully automated temperature control is accomplished starting from a preparation temperature of 2 °C with a cooling rate standardized to 1.5 ± 0.2 °C min^{-1}. A typical temperature profile of the cooling water droplet of 0.13 cm radius is presented in Fig. 2. A significant advantage of the method used is resolution of the latent heat pulse measured upon freezing. The time moment of the sharp change of the temperature profile curve indicates the freezing onset (nucleation), t_w, see Fig. 2. A freezing time offset takes place due to the time duration needed for the droplet crystallization. In our experiments it was always found that crystallization takes less time than nucleation. According to the classical theory of heterogeneous nucleation (Pruppacher and Klett, 1978) water freezing is initiated by ice germ formation. Therefore, the method developed in this study assumes the use of ice nucleation statistics starting as the moment of the freezing onset (nucleation). The temperature corresponding to the nucleation point of time will be treated below as the freezing temperature, T_f. Immersion of soot particles into water droplets leads to the displacement of the nucleation onset, t_w, to warmer temperatures (see Fig. 2).

The time dependence of the nucleation process is well described by the exponential decay law that allows the application of Poisson statistics to the freezing of a large ensemble of identical samples (Koop et al., 1997). Then, the

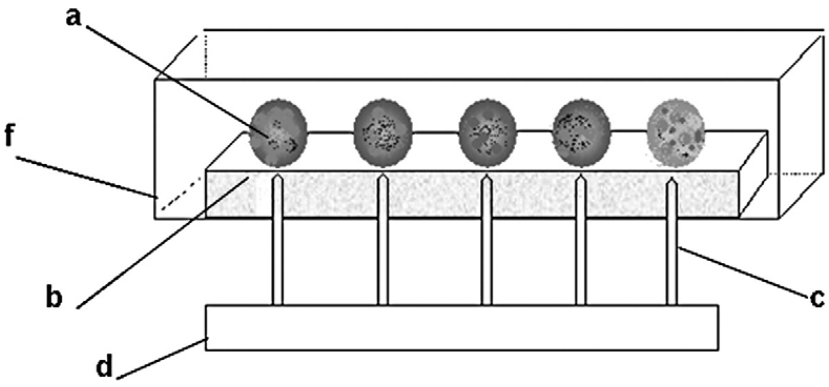

Fig. 1. Sketch of experiment setup: a) droplet, b) Teflon substrate, c) resistance temperature sensor, d) electrical thermometer, f) cooler.

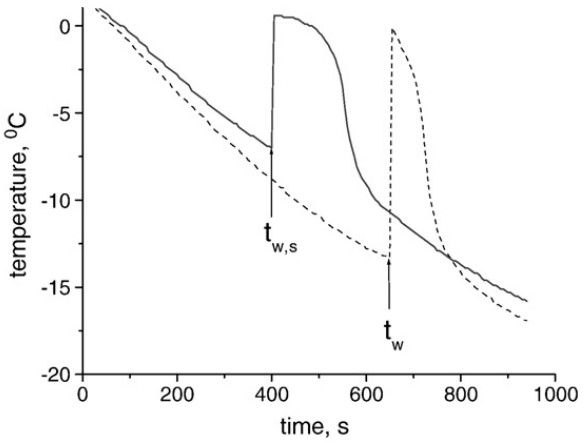

Fig. 2. Typical temperature profiles of the cooling/freezing water droplet.

probability that N_{un} droplets from N_o equal droplets do not nucleate within an observation time t is given by

$$P(t) = \frac{N_{un}}{N_o} \approx \exp(-Jt) \quad (1)$$

The approximation of Eq. (1) becomes more accurate as the number of sample droplets N_o is increased. We have analyzed the ensemble of 100 droplets for calculating of the nucleation rate J using Eq. (1).

A series of preliminary experiments was done to check the reliability of freezing results for pure water droplets of different sizes which ranged from 0.06 to 0.21 cm. The size of 0.13 cm radius was chosen as optimal for the experiments with soot suspensions because it allows the control of immersed soot mass, near 2.5 wt.%, with a good accuracy. We do not attempt measurements with higher soot mass because of uncontrolled sticking of soot particles to the dozator walls from the suspension of greater soot mass.

The water suspensions were prepared from original and sifted soot powders by gentle stirring. Following the Enrburger-Dolle et al. (1990) finding that the ultrasonic treatment does not change significantly the structure of furnace and acetylene soot agglomerates in water, we did not use unltrasonication. Because of the slow kinetics of soot interaction with the dispersing medium of water (wetting and settling) the freshly prepared suspensions were left for a few days, and afterwards were additionally stirred to produce the droplets that were subsequently frozen.

3.1. Preliminary freezing experiments

Theoretically, ice will nucleate homogeneously in supercooled water droplets under sufficient cooling. However, in experimental practice, microimpurities in distilled water and contact with the supporting surface can prevent the droplet from supercooling deeply. Fig. 3 A shows the percentage frequency of freezing of pure water droplets versus temperature for three ensembles of different sizes. For water droplets 0.13 cm radius a broad distribution of freezing temperature was observed, with the warmest T_f noted in the vicinity of −7 °C and the coldest of −16 °C. A clear dependence of T_f on the droplet size is observed: the smaller the droplet size the greater is the supercooling needed for freezing. This is in accordance with the well-known volume dependence of the median freezing temperature in the heterogeneous immersion freezing mode (Pitter and Pruppacher, 1973).

The freezing data from the experiments involving pure water droplets of 0.13 cm radius are presented in Fig. 4. Plotting the logarithm on the left side of Eq. (1) versus time, a straight line should be obtained, and the nucleation rate, J, is approximately equal to the negative slope of this straight line. Such a dependence was observed for homogeneous nucleation of small water droplets near 40 μm radius at $T \sim -37$ °C (Stockel et al., 2005). Our experimental points cannot be treated by one straight line (see Fig. 4). We therefore propose fitting two lines to the data assuming the existence of two fractions of droplets: one freezes early and slowly, the second one later and quickly. Such an assumption is based on experimental observations of a strong dependence of the

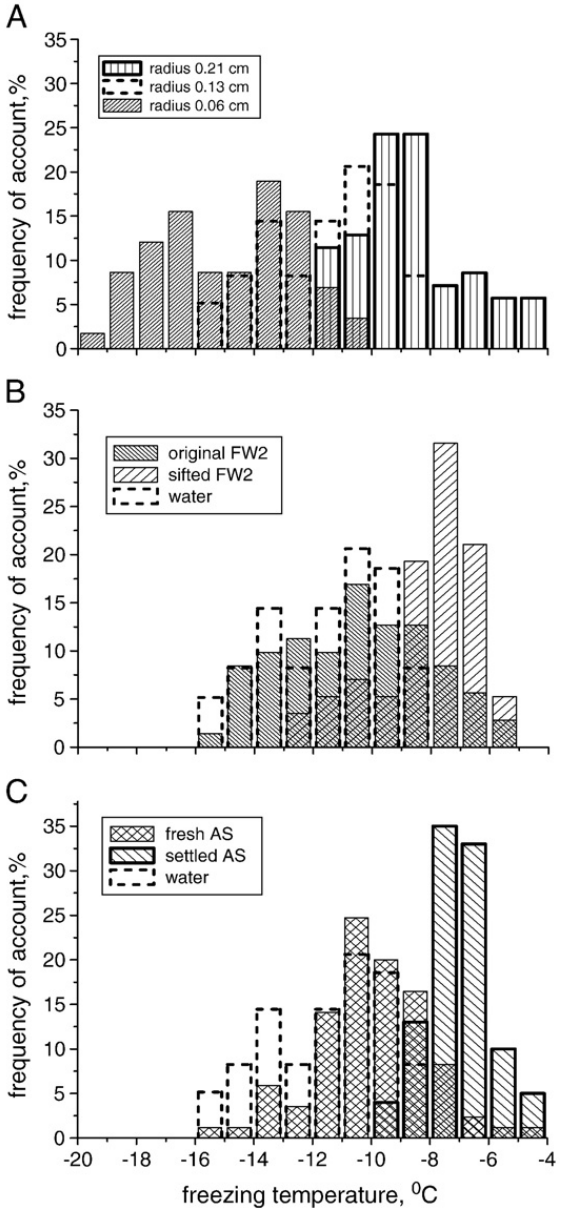

Fig. 3. Histograms of the freezing frequency of A) pure water droplets of radius 0.21, 0.13 and 0.06 cm, B) original and sifted freshly prepared suspensions of FW2 soot, and C) original freshly prepared and settled AS soot suspensions versus the freezing temperature. Radius of droplets in B) and C) cases is 0.13 cm.

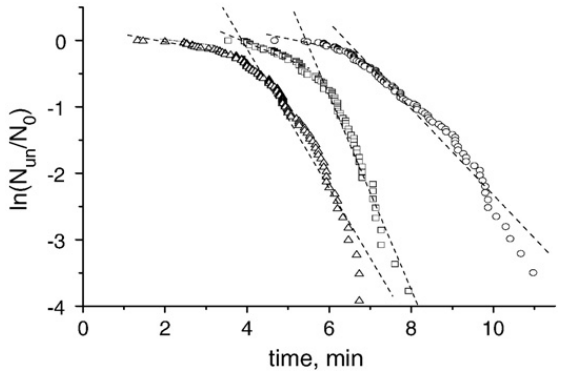

Fig. 4. ln (N_{un}/N_o) plotted versus time for pure water droplets (circles), water droplets with immersed original settled FW2 (squares) and AS (triangles) soots. Cooling rate is 1.5±0.2 °C min^{-1}.

number of ice germs formed in a droplet volume on supercooling in the temperature range near zero (Pruppacher and Klett, 1978, Ch.9). This finding supports the singular hypothesis of the water freezing mechanism (Pruppacher and Klett, 1978, Ch.9) assuming that the droplet freezing characteristics can be attributed to the nature of the surface active sites initiating the ice germ growth.

The medium freezing temperature, $\overline{T}_f$, for whole ensemble of pure water droplets of 0.13 cm radius is found to be −11.5 °C with the standard deviation 2.1 °C. The confidence interval is ±0.4 at 95% confidence level. The nucleation rates, J_1 and J_2, are determined by negative slopes of two straight lines fitting the experimental points respectively at the early and late times, they are found 0.1 and 0.6±0.01 min^{-1}. No sensitivity of these results to a change of cooling rate by a factor of two was observed within accuracy of these measurements.

4. Results and discussion

Literature on the ice-forming ability of insoluble particles in the direct deposition mode yields a number of requirements relating to size, microstructure, insolubility, chemical bond, and surface sites (Pruppacher and Klett, 1978). Soot particles immersed in large numbers into water droplet form a lyophobic dispersed system which is thermodynamically non-equilibrium due to significant abundance of free surface energy. This abundance causes the sedimentation instability of the system (sedimentation of particles under gravity) and aggregative instability (coagulation of particles to decrease surface free energy). Therefore, in addition to the requirements for direct deposition nucleation mode (Pruppacher and Klett, 1978), we have to take into account the specific features of soot behaviour in water (floating or sedimentation), coagulation of agglomerates, and kinetics of wetting.

4.1. Soot behaviour in water and freezing

4.1.1. Spatial distribution

Behaviour of soot in water is defined by the mass density of the soot agglomerates, the size of aggregates and wetting characteristics. Lamp Black, FW2 and Furnace Black soots are characterized by a high value of ρ_o (see Table 1), their particles sediment on the droplet bottom demonstrating the features of the "sedimentation instability" (SI). Fig. 5A shows the typical image of macroscopic water droplet with immersed FW2 soot. Acetylene soot (AS) having a low mass density creates a suspension with particles homogeneously distributed over droplet volume; these particles have the property of floating. In contrast to FW2, water droplets with AS soot are uniformly dark (see Fig. 5B).

The procedure of sifting the original soot powders with purpose to remove the large agglomerates (more than 80 μm) decreases the mass density of soot agglomerates for FW2 and LB soots (see Table 1) leading to the appearance of the sedimentation stable (SS) suspension. For FW2 soot ρ_o decreases by a factor of two, and one sees uniformly dark water droplet in Fig. 5C.

Histograms of the freezing frequency of droplets versus the temperature are shown in Fig. 3B for original and sifted FW2 soot in freshly prepared suspensions. The coldest and warmest temperatures, and median freezing temperatures $\overline{T}_f$ are found to be warmer than in water droplet measurements. We will term the displacement of the median freezing temperature with respect to pure water by the *freezing efficiency*, $\overline{\Delta T}_f$. At the 95% confidence level (using a *t*-test) the difference of freezing temperatures between water and soot suspensions is significant for all considered cases with exceptions of freshly prepared AEC and T-900 original suspensions, T-900 sifted suspension, and settled furnace and T-900 sifted suspensions.

The sifted FW2 particles that distribute homogeneously through the droplet volume stimulate more efficient freezing; $\overline{\Delta T}_f$ for this SS suspension is found to be 3.4 °C, while $\overline{\Delta T}_f$ for the SI suspension of original soot is 0.9 °C. A similar effect is observed for LB soot (see Table 3) indicating that the distribution of soot particles over droplet volume plays a significant role in the freezing phenomenon; heterogeneous freezing, which is nearly indistinguishable from unseeded water drop freezing, takes place in the sedimentation stable suspensions, whereas floating particles stimulate freezing of the water droplet more efficient than settled particles.

However, decrease of the mass density is not the sufficient condition for changing the particle distribution over the droplet. The cutoff of the large agglomerates of AS and FB soots does not change the floating properties of its particles; we observe SS and SI suspensions in both original and sifted soot suspensions, respectively for AS and FB soots.

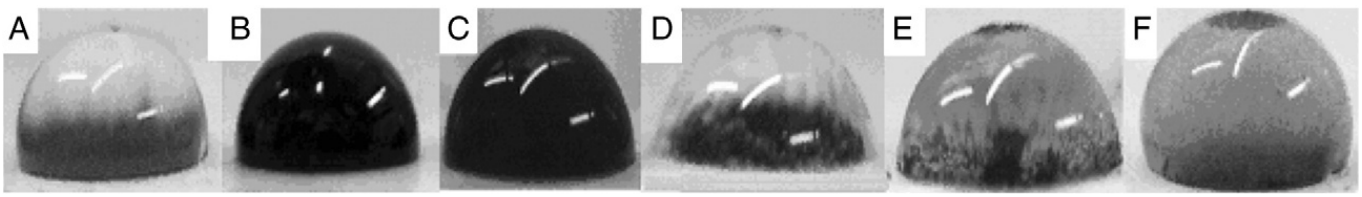

Fig. 5. Images of macroscopic water droplets with immersed particles of A) and B) original FW2 and AS soots, C) and D) sifted FW2 and FB soots, E) and F) original TC1 and AES soots, respectively.

Table 3
Medium freezing temperatures, °C, of water droplets with soot immersed

	Original soot suspension		Sifted soot suspension	
Type of soot	Freshly prepared	Settled	Freshly prepared	Settled
LB	SI	SI	SS	SS
	−9.8±1.8	−10.8±2.0	−7.6±1.0	−8.3±1.6
FB	SI	SI	SI	SI
	−8.2±1.6	−7.8±1.6	−7.3±1.4	−11.5±2.4
FW2	SI	SI	SS	SS
	−10.6±2.4	−9.9±2.3	−8.1±1.8	−9.0±2.0
AS	SS	SS	SS	SS
	−10±1.9	−7.1±1.1	−6.8±1.8	−6.8±1.6
T-900	SI	SI	SI	SI
	−11.9±1.9	−10.1±2.2	−11.1±2.4	−11.9±2.5
AEC	SI	SI		
	−11.1±2.3	−10.6±2.2		

Stability of suspension is indicated.
$\overline{T}_f$ for pure water droplets of 0.13 cm radius is −11.5±2.1 °C.

Additionally, there is a correlation between wetting ability of the soot surface and the floating properties of soot agglomerates. For a given mass density, soot characterized by a smaller contact angle is more wettable and therefore its particles more easily sediment to the droplet bottom. As an example, FW2 and FB soots have the similar ρ_s for sifted soot (see Table 1), but in the first case we observe the dark droplets of SS suspensions (see Fig. 5C) while in the latter case the typical image of SI suspension occurs (see Fig. 5D). This result correlates to the low contact angle for FB soot (28°), in comparison to FW2 soot (40°).

4.1.2. Effect of settling

Soot is a highly porous material (see Table 1), but in the case of large agglomerates of original soot immersed into water, a significant part of their total specific surface area is not accessible for water interaction. It takes time for water molecules to penetrate intra-aggregate voids, then inter-aggregate and interparticle cavities, and inside-particle micropores. Finally when the surface area accessible to water increases, for example as the soot suspensions settle over a few days, a warmer freezing temperature results occurs. Table 3 presents $\overline{T}_f$ for freshly prepared and settled suspensions of original soots. One can see this wetting kinetics effect for nearly all soots used in this study. The most prominent impact of wetting kinetics, an increase in freezing efficiency of 2.9 °C (see histograms in Fig. 3C), is observed for AS soot, probably because this soot has the highest porosity. We speculate that the highest volume of empty voids between aggregates allows water molecules to interact with the larger part of the surface. However, we note that even after a few days of settling the total surface area of soot agglomerates is not accessible to water, which is clear from the comparison of $\overline{T}_f$ for FW2 soot with large surface area (S=420 m^2/g) and for T-900 with low surface area (S=10 m^2/g).

Sifting the soot powder significantly decreases the size of agglomerates dispersed in water and increases the surface area acceptable for water. This is why with well-dispersed particles we observe the increase of $\overline{T}_f$ in general for all soots. But the largest effect, $\overline{\Delta T}_f \approx 4.7$°C, is found for AS soot suspension (see Fig. 3C). Probably, its agglomerates are easily breakable by gentle stirring, as it was noted in Ehrburger-Dolle et al. (1990). In addition, AS agglomerates are well "structured and branched" as one can see the optical image of sifted AS soot in water in Fig. 6A. In contrast, for instance, LB soot agglomerates demonstrate a globular structure of larger size (see Fig. 6B), and during settling some of them coagulates forming black patches.

Sifting the soot aggregates increases the total free energy of the suspension; it may lead to the aggregative instability of a given system. The phenomenon of a changing the soot particle size spectrum in water and a tendency to form clusters was observed by Diehl and Mitra (1998). Settling of sifted soots during a few days decreases $\overline{T}_f$ (see Table 3) because of the coagulation between dispersed soot agglomerates resulting in the decrease of the total wetted surface area. The most significant effect of coagulation on the freezing efficiency is observed for FB soot, 4.2 °C, the sedimentation instability of its suspension may stimulate aggregate coagulation.

4.1.3. Behaviour of TC1 and AEC soots

The mass density of TC1 soot particle collected samples is the lowest among soots studied but the contact angle is the highest (see Table 1); a significant number of their particles concentrated on the top of water droplet as found before in Demirdjian et al. (2007). Frequently these "top" particles appear to be externally mixed with water because some particles are "shoved out" onto the surface (see Fig. 5E), possibly due to the pure wettability of the surface. Because of such behaviour we could not prepare fresh droplets with controlled soot mass; only after a few days settling could the suspension be used. The mean freezing temperature for TC1-O soot was −10.2±2.1 °C, which is closer to that of pure water (just 1.3 °C higher).

In contrast, AEC soot has the highest number mass density but we found particles both on the bottom and the top of

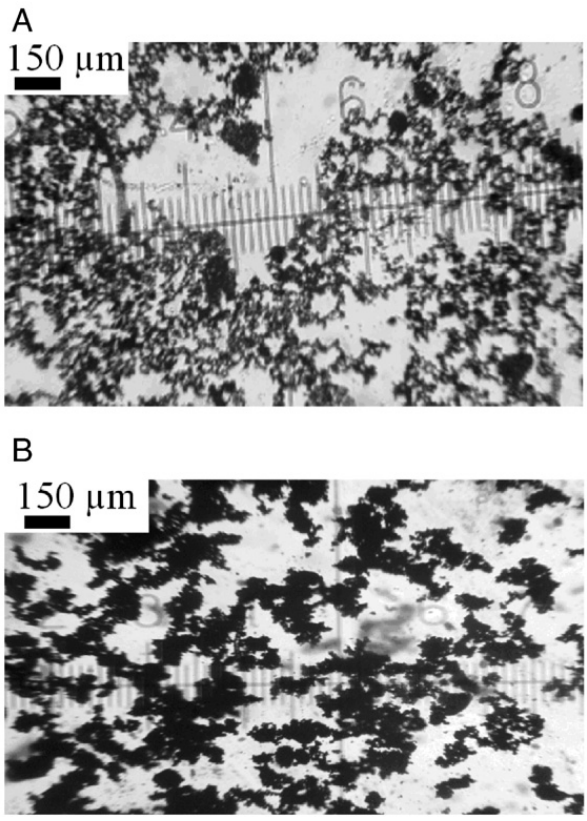

Fig. 6. Optical images of sifted A) AS and B) LB soot in water.

droplets (see Fig. 5F). Such behaviour is in correlation with Popovicheva et al. (2004) finding that AEC soot particles may be separated into two fractions: hydrophobic fraction similar to TC1 soot and hydrophilic fraction with soluble impurities. The hydrophobic fraction probably accumulates on the top droplet surface, similar to TC1 soot, whereas the other fraction that sediments to the bottom surface of the droplet is likely the hydrophilic fraction with soluble impurities. Even after suspension settling, low $\overline{T}_f \sim -10.6$ °C is found because of the low porosity of original AEC (see Table 3). Thus, the results indicate poor heterogeneous ice nucleation ability of densely packed soot distributed over the surface.

By examining cases of similar distribution of particles of different soot over water droplet volumes, the impact of surface properties such as wetting, level of polarity, amount of active sites, and solubility can be considered. These impacts will be discussed in next sessions.

4.2. Wetting and freezing

Supercooled liquid water which contains solid particles may freeze at temperatures significantly higher than the homogeneous nucleation point because of increases in the free energy of the system due to formation of an ice embryo on an ice nucleating particle surface (Pruppacher and Klett, 1978, Ch9). According to the classical Fletcher theory the ice nucleation efficiency and nucleation rate are highly sensitive to the contact angle parameter, θ (Fletcher, 1958, 1959a,b). Quantitative agreement with the observed dependence of heterogeneous immersion freezing temperatures in experiments with mineral dust particles has been achieved by assuming a distribution of wetting parameters (Hung et al., 2003; Marcolli et al., 2007).

In the immersion freezing mode, the required supercooling decreases rapidly with increasing θ. Thus, the temperature at which the ice germ nucleates on a spherical particle of more 100 μm in one second is increased by 10 °C at the changing of θ from 40 up to 28° (Pruppacher and Klett, 1978, Ch.9). Such sensitivity was not observed in our experiments; for example, for FW2 and FB original settled soots we obtained a difference only of two degrees between freezing temperatures (see Table 3). For AS and T-900 soots having similar θ we found a freezing temperature difference of three degrees. Moreover, we identify two nucleation rates, for early and later freezing droplets (see Fig. 4); and both rates are found approximately a factor of two or three more than for pure water droplets. Thus, we may only report the qualitative dependence of $\overline{T}_f$ on wetting parameter.

The above discrepancy arises from a number of serious limitations coming from the simplicity of the classical theory of heterogeneous nucleation on spherical particles. One of them is that soot agglomerates are highly porous: inter-aggregate, interparticle mesopores and inside-particle micropores are cavities of confined size. The phenomenon of supercooling of confined water was observed in glass (Bellissent-Funel et al., 1995), in charcoal powder (Bellissent-Funel et al., 1996), and in kerosene soot (Ferry et al., 2002). Thermoporometry measurements of the lowering of the triple point temperature of water with immersed acetylene soot from 0.6 °C to 1.7 °C lead to estimates of a minimum ~39 nm and maximum ~109 nm radius of the intra-aggregates voids (mesopores) (Enrburger-Dolle et al., 1990). Therefore, together with an effect of the spherical surface of particles we should consider the impact of negative curvature between particles assuming that the soot with higher mesoporosity may lower freezing efficiency. Thus, the volume of mesopores obtained for FW2 and LB soots are found to be 0.9 and 0.05 cm^3/g, respectively. Such a difference is due to the significantly smaller size of primary FW2 soot particles and the lager surface area of this soot in comparison with LB soot (see Table 1). However, we don't see a significant difference between $\overline{T}_f$ for FW2 and LB soots, neither in original settled nor in sifted suspensions. The same finding applies to other soots. The volume of micropores is much less than the volume of mesopores. For example, it is ≈0.02 cm^3/g for TC1-O soot. This is why the supercooling of water in micropore and mesopores is expected to have no impact on freezing temperature in our experiments.

4.3. Hydration and freezing

Soot wetting ability in general correlates to its hydrophilicity which may be characterized by measurements of water uptake from the gaseous phase (Persiantseva et al., 2004). The fundamental theory of water adsorption on carbonaceous adsorbents assumes that due to low dispersion energy between water molecules and carbon there is a strong dependence on the presence of hydrophilic oxygen-containing sites, so called primary adsorption sites (Dubinin, 1980). Table 1 shows that the oxygen content of soots generally correlates with volatile organic coverage and wetting parameter when total surface area differences are accounted for. These data suggest the greater hydrophilicity of FB and FW2 in comparison with T-900 and AS soots.

Fig. 7A shows the isotherms of the water adsorption measured on LB,FB,FW2,AS,CRS and T-900 soots as a function of the relative humidity (RH). A correct comparison, absolute adsorption isotherms calculated per unit of surface area are presented using the measured values of the surface areas reported in Table 1. One statistic monolayer of water, 1 ML, calculated assuming an effective molecular cross-section area for the water molecule of 0.105 nm^2, is also indicated. A loose packed continuous monolayer of water may not form on soot surfaces due to preferable adsorption on the active oxygen-containing sites (Dubinin, 1980) following water cluster formation (Muller et al., 1996). Nevertheless, this value is proposed as a reference to characterize the level of the soot polarity in comparison with amount of water adsorbed at 50% RH (Carrott, 1992; Persiantseva et al., 2004).

AS soot is found to be the most hydrophobic among all soots; it is characterized by negligible adsorption at the initial RH in correlation with very low oxygen content, chemical and structural homogeneity of its surface (Kiselev and Kovaleva, 1965). Water adsorption on T-900, LB and FW2 soots is significantly higher over whole RH range. Their isotherms are concave at low RH which is a feature of the presence of active sites accessible for water adsorption. Nevertheless, the amount of water adsorbed still does not approach 1 ML at 50%RH, so these soots may be characterized as relatively hydrophobic with surfaces of low polarity. FB soot is found to be the most hydrophilic in this group of relatively hydrophobic soots; its isotherm is typical for a surface of intermediate polarity.

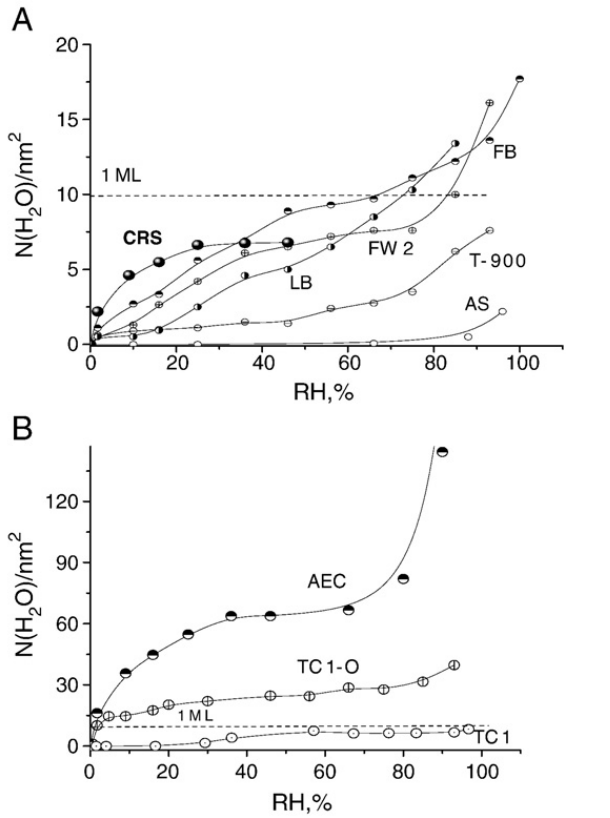

Fig. 7. Amount of water molecules per nm^2 versus the relative humidity on A) AS, T-900,LB,FW2, FB and CRS soots and on B) TC1, TC1-O, and AEC soots at T=295 K. One statistic monolayer of water, 1 ML, is indicated. Uptake on CRS as the most effective immersion freezing IN is marked by large dark symbols.

A convex shape of the isotherm allows the estimation of the number density of primary active sites, a_m, (Vartapetyan and Voloshchuk, 1995) by applying the BET theory to water adsorption data (Gregg and Sing, 1982) assuming that in the range of low RH up to 20% one water molecule is adsorbed on each primary site. The value of a_m obtained per unit of surface is present in Table 2. One can see the correlation between the number density of active sites, level of the surface polarity and wetting ability. High $a_m \approx 4.2$ nm^{-2} is found for FB soot characterized by low contact angle ~28°. Then, the part of the surface available for water, S_{H2O}, may be estimated as ≈63 m^2/g. By calculating the ratio of S_{H2O} to total surface S we find that 60% of the total surface of FB soot may be considered as hydrophilic and the reminder as hydrophobic. Other relatively hydrophobic soots in this group have smaller S_{H2O}/S ratio.

Experiments reviewed in Pruppacher and Klett (1978, Ch.9) have established that heterogeneous ice nucleation proceeds at active sites. It was assumed that sites which are capable of adsorbing water molecules are also sites at which ice nucleation is initiated while the number of critical embryos per unit area of the substrate is proportional to the number of water molecules adsorbed per unit area. Therefore it is reasonable to accept the singular hypothesis for the freezing mechanism and it appears consistent to note the highest $\overline{T}_f$ in this group for FB soot, equal to −7.8 °C, while others soots have lower $\overline{T}_f$ in correlation with smaller a_m and wetting ability (see Table 3 for original settled suspensions). Thus, we infer the largest effect on freezing from the most hydrophilic soot (in this group).

Hydrophilic heterogeneities like the active sites on hydrophobic surfaces can produce beneficial effects regarding the ice nucleation potential; the phenomenon suggested for silver iodide by Zettlemoyer and McCafferty (1973). It was pointed out by Fletcher (1959b) that a low-polar surface has an advantage in ice nucleation. A polar substrate is a poor nucleation agent because it orients ice dipoles parallel to one another, and therefore it raises the free energy of formation of embryos grown upon it. Therefore, the surface of relatively hydrophobic soots with hydrophilic nucleation sites surrounded by a hydrophobic region may be considered as providing the best conditions for heterogeneous freezing. Then, the growth of ice embryos is facilitated by the surface diffusion of weakly adsorbed molecules from the liquid to the active sites, the phenomenon similar to the growth of a cluster on the previously adsorbed water molecules from vapor phase.

Nevertheless, comparative analysis of the freezing efficiency indicates that a correlation with extent of hydrophilicity is justified only for the suspensions of similar particle behaviour (as for SI suspensions in the case above). The fact that a stable homogeneous soot particle distribution gives high $\overline{T}_f$=−7.1 ± 1.1 °C even for hydrophobic AS soot suggests that if more hydrophilic soot establishes a homogeneous particle distribution we may obtain higher $\overline{T}_f$ than for hydrophobic soot (hypothetic summary effect).

Laboratory-made TC1-O kerosene flame soot is characterized by a higher water adsorption than previous group of soots. It starts to adsorb water at low RH (see Fig. 7B), a typical feature of adsorbents with the large fraction of hydrophilic heterogeneities (Gregg and Sing, 1978). For a_m we found 15 nm^{-2} .This value reveals that the entire surface is available for monolayer water coverage already at low RH ~ 10%. But $\overline{T}_f$ for TC1-O soot was warmer than that of pure water by only 1.3 °C. The reason for this result may be that its particle distribution over the droplet surface prevents freezing because some part of particles appears are not wettable and do not participate in freezing (see Fig. 5E). More likely, the surface of TC1-O soot is totally covered by polar heterogeneities: water molecules likely bound into the monolayer and lose their freedom for the orientation needed for ice-like structure formation (Pruppacher and Klett, 1978, Ch.9). This contrasts with water molecules joined together to form clusters on relatively hydrophobic soot surfaces that have considerable freedom to move their dipoles into an orientation most favorable for ice arrangement.

To check the inferred hypothesis we examined the water uptake ability of previously produced TC1 soot and found that its isotherm is lower than that of oxidized TC1-O soot (see Fig. 7B), the number density a_m is much lower in correlation with less oxygen content (see Table 1), amount of water adsorbed is totally much less than 1 ML. For this TC1 soot we found $\overline{T}_f$=−9.3 ± 1.4 °C, higher by 1.1 °C than for TC1-O soot. This supports the conclusion that a low-polarity surface has an advantage in ice nucleation.

Finally we should note that the chemical nature of the active site for ice nucleation is also an important question. The ice-forming activity depends on the surface concentration of chemical groups that can form hydrogen bonds with water molecules (Gorbunov et al., 2001). However, the real surface of combustion particles is highly heterogeneous with respect to different functional groups, including oxygen-containing ones (Akhter et al., 1991). IR analysis found the presence of carboxylic

and aromatic C=O groups in FW2 soot (Kirchner et al., 2000), and carbonyl, phenol and hydroxyl groups in TC1 and combustor soots (Popovicheva et al., 2003b). The identification of the role of each of these requires a more elaborated spectral approach for production of soot with a surface coverage by a specific chemical nature.

4.4. Impact of water solubles

Surface active sites may be bonded with the carbon matrix or originate from compounds that cover the surface. However, if the soot surface is covered by water soluble inorganic and organic material, it is reasonable to assume that active sites may be vulnerable to dissolution after a particle has become immersed in water. Then we may predict the reduction of potential ice nucleation ability for really hygroscopic soot.

The water soluble fraction found in the different samples of the *Set of soots* varied from 0.3 up to 13.5 wt.% (see Table 2); that is in a general correlation with extent of soot hydrophilicity. WSF could not be measured for really hydrophobic AS soot. AEC soot demonstrates higher hygroscopicity in accordance with 13.5 wt.% of WSF as evidenced by significant water adsorption already at very low RH (see Fig. 7B). Calculation of the water amount corresponding to one monolayer gives $a_m \approx 42$ nm^{-2} and $S_{H2O}/S \approx 5$, indicating that the total surface of AEC soot of high polarity is covered by five monolayers of water at 20%RH. This amount of water may be accumulated on hygroscopic soot only if the dissolution of water in soluble surface material is possible.

Additionally, the WSF of AEC soot contains 3.5 wt.% of sulphates which are easily washed by water as it was demonstrated by FTIR analysis in Popovicheva et al. (2004). The mechanism of the dissolution of water molecules in the soluble coverage of hygroscopic soot is different from the bonding into clusters near active sites of relatively hydrophilic soot. It prevents the formation of ice-like structure and appears to be responsible for the low $\overline{T}_f \approx -10.6$ °C for AEC soot. It is possible that even 1 wt.% of the WSF, as found for TC1-O soot, is enough to form on the surface a few monolayers of water solution that inhibits the freezing. Therefore it is possible to infer that the high hygroscopicity of soot is not favourable for nucleation efficiency in the immersion freezing mode. However, in the case of activated cloud droplets for which the solute concentration can be highly and rapidly diluted freezing may take place on the "washed" surface with modified properties. It may lead to the different freezing ability since the surface will loose its WSF.

Finally, to attempt to prove the hypothesis about the highest impact of the surface of intermediate polarity we have measured the water uptake and freezing efficiency of oxidized CRS soot. The clear convex isotherm indicates the high number density of active sites, ~6.3 nm^{-2}, but the surface of this soot is still relative hydrophobic (see Fig. 7A). The highest $\overline{T}_f \approx -6.8 \pm 1.5$ °C found for SI suspension of CRS soot confirms that it is the most effective immersion freezing IN among the other soots examined in this work.

5. Conclusions

The advantage of the approach elaborated in this work is a large variety of characterized properties represented in the *Set of soots*; that may offer indications of important properties for potential atmospheric ice nuclei. A list of key soot characteristics relating to the immersion freezing efficiency was obtained. In the present study, conditions leading to a homogeneous distribution of the high mass soot particles through drops promoted the largest displacement of freezing temperature compared to unseeded water drops. The uniformity of the soot particle distribution in drops is controlled by the mass density of the composite soot particle, the size of agglomerates and the wetting properties of the soot surface. We suggest that these factors must be considered as additional requirements for immersion freezing of large (~1 μm diameter) soot particles, together with the wetting parameter and number of active sites. Accumulation of soot particles on the droplet bottom due to sedimentation instability or on the droplet surface due to a poor wettability limits the efficiency of the heterogeneous freezing.

A surface of large size and low porosity agglomerates will not be totally wetted within water droplets or haze droplets, small primary particle and structural agglomerates are preferable for ice nucleation. Therefore, our results could be considered as limiting values obtained for a finite surface. The highest effect may be predicted from separate aggregates and primary particles. Thus the accessible soot surface is also an important requirement; one that may partly be achieved by long time residence of soot in water. In contrast, the aggregate instability of polluted or large soot mass suspensions with small size agglomerates inhibits the ice nucleation. This may play a significant role in limiting ice nucleating, especially, if it is enhanced by the sedimentation instability.

The extent of soot hydrophilicity, for soots that are overall relatively hydrophobic, is the second main characteristics relating to immersion freezing efficiency. A gradual increase of the freezing temperature in correspondence with amount of active oxygen-containing sites is observed for relatively hydrophobic soots having surfaces of low or intermediate polarity. Quantitatively, we may add the maximum efficiency obtained for CRS soot, $\overline{\Delta T}_f = 4.7$°C, to $\overline{\Delta T}_f = 4.7$°C found for a homogeneous suspension of hydrophobic AS soot forming homogeneous suspension, and conclude a highest effect of 9.4 °C for the best immersion freezing nuclei which may be hypothesized on the bases of our experimental results.

However, the hydrophilicity requirement may not be extended to soots with large soluble fractions present on their surfaces. Soluble coverage changes the mechanism of water uptake from water cluster growth on the active sites to the dissolution into soluble surface material. Hydrophilic nucleation sites surrounded by a hydrophobic surface have an advantage for the growth of ice germs while functional groups originating from soluble compounds reduce the potential ice nucleability. Therefore our results predict that soot particles with surfaces of low to intermediate polarity having a significant number of oxygen-containing functional groups, but in concentrations less than needed for forming a water monolayer coverage at 50%RH, are the best candidates as atmospheric soot IN. In other words, the surface should not be covered totally by hydrophilic sites due to high oxidation or because of the present soluble organic/inorganic sulfate compounds.

6. Atmospheric application

The relevance of this study for cloud physics concerns airborne water droplets nucleating in the presence of soot particles which may enter the droplet prior to freezing either by cloud scavenging or by droplet formation on these particles serving a cloud condensation nuclei (CCN). The simplest situation in the first scenario is the case of micron-size droplet scavenging one primary particle or one aggregate of primary particles, i.e. the case of the water volume limited by the particles motion and interaction between each other, not nucleation scavenging. In this situation the properties responsible for the extent of soot hydrophilicity (oxygen content, number of functional groups, and soluble fraction) will play a significant role. The maximum potential freezing efficiency may be proposed as even more than 10 °C, because in this case the total surface area of the soot particle will be involved in the nucleation process.

Based on our results, neither really hydrophobic soot with extremely low oxygen content (probably total elemental carbon) nor highly hygroscopic soot having a large soluble coverage may impact ice nucleation in the immersion freezing mode. Surface polarity of different soots from various combustion sources should be analyzed with regard to the most effective extent of hydrophilicity supporting the mechanism of ice germ growth on hydrophilic nucleation sites. Hence, the question of how the nucleation efficiency depends on combustion conditions (and as consequence on surface coverage of the condensable combustion products) becomes clearer.

Soot aging plays a potential role in ice nucleation because the coagulation with soluble aerosols, condensation of oxidized gases and photochemical processes may lead to the transformation of hydrophobic to hygroscopic soot particles (Riemer et al., 2004; Hendricks et al., 2004). Already 1 wt.% of water soluble compound may change the extent of hydrophilicity while 5 wt.% means the appearance of internally mixed aerosol (Riemer et al., 2004). The hygroscopic pathway is the most likely way that soot particles get immersed in cloud drops. If hygroscopicity of soot particles inhibits their ability to act as ice nuclei that would appear to diminish their role as effective ice nuclei in the atmosphere, an important result.

The second scenario of soot particles interacting with clouds assumes a two-stage process, in that condensation must first occur, following by freezing (Fletcher, 1958). Then, soot particles should act first as CCN and initiate the immersion freezing nucleation upon further cooling of droplets. However, the high CCN activity of soot particles requires a large water soluble fraction (Hallet et al., 1989; Lammel and Novakov, 1995) and this characteristic is qualitatively associated with poor immersion freezing efficiency in our work. Probably, high WSF was the reason for low fraction of acetylene soot nucleated as ice with respect to the number of aerosols immersed in cloud droplets effectively formed by these particles before strong cooling in DeMott (1990). High WSF near 23 wt.% measured for such kind of soot in Hallet et al. (1989) may serve as a prove.

In view of these findings, the hygroscopic fraction of impurities in aircraft engine generated soot may uptake water in the cooling plume (Popovicheva et al., 2004) and serve as good CCN at saturation conditions but may not initiate the ice nucleation by immersion freezing due to effective dissolution of water in its soluble surface coverage. Thus, it appears necessary to approach water saturation or greater in the plume to freeze the forming droplets. In opposite, the hydrophobic main fraction, even if it may be activated by plume proceeding (Shonija et al., 2007), may be not a good CCN and therefore, again we assume that water supersaturations must occur in the plume before freezing can occur we should assume the water supersaturation in the plume first for the freezing after. These conclusions are in the good correlation with observations of the threshold contrail formation conditions (Kärcher et al., 1998) showing the necessity of achievements of water supersaturation in the plume.

Acknowledgements

This research is funded by EU FP6 Project QUANTIFY-TTC 003893, the grant of President of Russian Federation SS-133.2008.02 and Project ISTC 3097. Some remarks and conclusions assisted by one of the reviewers are acknowledged.

References

Akhter, M.S., Chughtai, A.R., Smith, D.M., 1991. Spectroscopic studies of oxidized soots. Appl. Spectr. 45, 6563–6665.
Bellissent-Funel, M.-C., Chen, S.H., Zanotti, J.-M., 1995. Single-particle dynamics of water molecules in confined space. Phys. Rev. E 51, 4558–4568.
Bellissent-Funel, M.-C., Sridi-Dorbez, R., Bosio, L.J., 1996. X-ray and neutron scattering studies of the structure of water at a hydrophobic surface. Chem. Phys. 104, 10023–10029.
Carrott, P., 1992. Adsorption of water vapor by non-porous carbons. Carbon 50, 201–205.
Chen, Y., Kreidenweis, S.M., McInnes, L.M., Rogers, D.C., DeMott, P.J., 1998. Single particle analysis of ice nucleating aerosols in the upper troposphere and lower stratosphere. Geophys. Res. Lett. 25, 1391–1394.
Demirdjian, B., Ferry, D., Suzanne, J., Popovicheva, O.B., Persiantseva, N.M., Shonija, N.K., 2007. Heterogeneities in the microstructure and composition of aircraft engine combustor soot: impact on the water uptake. J. Atmos. Chem. 56, 83–103.
DeMott, P., 1990. An exploratory study of ice nucleation by soot aerosols. J. Appl. Meterol. 29, 1072–1079.
DeMott, P., 2002. Laboratory studies of cirrus cloud processes. In: Cirrus, D.K., Lync, et al. (Eds.), Chapter 5. Oxford University Press, New York, pp. 102–135.
DeMott, P.J., Rogers, D.C., Kreidenweis, S.M., 1997. The susceptibility of ice formation in upper tropospheric clouds to insoluble aerosol components. J. Geophys. Res. 102 (D16), 19575–19584.
DeMott, P.J., Chen, Y., Kreidenweis, S.M., Rogers, D.C., Sherman, D.E., 1999. Ice formation by black carbon particles. Geophys. Res. Lett. 26, 2429–2432.
DeMott, P.J., Cziczo, D.J., Prenni, A.J., Murphy, D.M., Kreidenweis, S.M., Thomson, D.S., Borys, R., Rogers, D.C., 2003. Measurements of the concentration and composition of nuclei for cirrus formation. PNAS 100, 14655–14660.
Diehl, K., Mitra, S.K., 1998. A laboratory study of the effects of a kerosene-burner exhaust on ice nucleation and the evaporation rate of ice crystals. Atmos. Environ. 32, 3145–3151.
Dubinin, M.M., 1980. Water vapor adsorption and the microporous structure of carbonaceous adsorbents. Carbon 18, 355–364.
Dubinin, M.M., Stoeckli, H.F., 1980. Homogeneous and heterogeneous microspore structure in carbonaceous adsorbents. J.Colloid Interface Sci. 75, 34–42.
Dymaska, M., Murray, B.J., Sun, L., Eastwood, L., Knohf, D.A., Bertram, A.K., 2006. Deposition ice nucleation on soot at temperatures relevant for the low troposphere. J. Geophys. Res. 111, D04204. doi:10.1029/2005JD006627.
Enrburger-Dolle, F., Misono, S., Lahaye, J., 1990. Characterization of the aggregate void structure of carbon blacks by thermoporometry. J. Colloid Interface Sci. 135, 468–485.
Ferry, D., Suzanne, J., Nitsche, S., Popovicheva, O.B., Shonija, N.K., 2002. Water adsorption and dynamics on kerosene soot under atmospheric conditions. J. Geophys. Res. 107, 4734–4744.
Fletcher, N.H., 1958. Size effect in heterogeneous nucleation. J. Chem.Phys. 29, 572–576.

Fletcher, N.H., 1959a. On ice-crystal production by aerosol particles. J. Meteorol. 16, 173–180.
Fletcher, N.H., 1959b. Entropy effect in ice crystal nucleation. J. Chem. Phys. 30, 1476–1482.
Gierens, K., 2003. On the transition between heterogeneous and homogeneous freezing. Atmos. Chem. Phys. 3, 437–446.
Gorbunov, B., Baklanov, A., Kakutkina, N., Windsor, H.L., Toumi, R., 2001. Ice nucleation on soot particles. Aerosol Sci. 32, 199–215.
Gregg, S.J., Sing, K.S.W., 1982. Adsorption, Surface Area and Porosity, 2nd ed. Academic Press, NY.
Jensen, E.J., Toon, O.B., 1997. The potential impact of soot particles from aircraft exhaust on cirrus clouds. Geophys. Res. Lett. 24, 249–252.
Haag, W., Karcher, B., Strom, J., Minikin, A., Lohmann, U., Ovarlez, J., Stohl, A., 2003. Freezing thresholds and cirrus formation mechanisms inferred from in situ measurements of relative humidity. Atmos. Chem. Phys. 3, 1791–1806.
Hallet, J., Hudson, J.G., Rogers, C.F., 1989. Characterization of combustion aerosols for haze and cloud formation. Aerosol Sci. Tech. 10, 70–83.
Hendricks, J., Karcher, B., Dopelheuer, A., Feichter, J., Lohmann, U., Baumgartner, D., 2004. Simulating the global atmospheric black carbon cycle: a revisit to the contribution of aircraft emissions. Atmos. Chem. Phys. 4, 2521–2541.
Hoffer, T., 1961. A laboratory investigation of droplet freezing. J. Meteorol. 18, 766–776.
Hung, H.-M., Malinowski, A., Martin, S., 2003. Kinetics of heterogeneous ice nucleation on the surfaces of mineral dust cores inserted into aqueous ammonium sulfate particles. J.Phys. Chem. A. 107, 1296–1306.
Kärcher, B., Peter, T., Biermann, U.M., Schumann, U., 1996. The initial composition of jet condensation trails. J. Atmos. Sci. 53, 3066–3083.
Kärcher, B., Busen, R., Petzold, A., Schröder, F., Schumann, U., Jensen, E.J., 1998. Physicochemistry of aircraft-generated liquid aerosols, soot, and ice particles — 2. Comparison with observations and sensitivity studies. J. Geophys. Res. 103, 17129–17147.
Kiselev, A.V., Kovaleva, N.V., 1965. Adsorption properties of acetylene soot. Russ. Colloid J. XXVII, 822–826.
Koop, T., Luo, B., Biermann, U., Crutzen, P., Peter, T., 1997. Freezing of HNO_3/H2SO4/H2O solutions at stratospheric temperatures: nucleation statistics and experiments. J. Phys. Chem. A. 101, 1117–1133.
Koop, T., Ng, H.P., Molina, L.T., Molina, M., 1998. A new optical technique to study aerosol phase transition: the nucleation of ice from H_2SO_4 aerosols. J. Chem. Phys. A. 102, 8924–8931.
Kuhn, M., Petzold, A., Baumgardner, D., Schröder, F., 1998. Particle composition of a young condensation trail and of upper tropospheric aerosol. Geophys. Res. Lett. 25, 2679–2682.
Kantro, D., Brunauer, S., Copeland, L.E., 1967. The solid – gas interface. Vol.1, Ch. XII. Marcel Dekker, Inc., New York.
Kirchner, U., Scheer, V., Vogt, R., 2000. FTIR spectroscopic investigation of the mechanism and kinetics of the heterogeneous reactions of NO_2 and HNO_3 with soot. J. Phys. Chem. A. 104, 8908–8915.
Lammel, G., Novakov, T., 1995. Water nucleation properties of carbon black and diesel soot particles. Atmos. Environ. 29, 813–823.
Lohmann, U., Karcher, B., Hendricks, J., 2004. Sensitivity studies of cirrus clouds formed by heterogeneous freezing in the ECHAM GCM. J. Geophys. Res. V. 109, D16204. doi:10.1029/2003JD004443.
Marcolli, C., Gedamke, S., Zobrist, B., 2007. Efficiency of immersion mode ice nucleation on surrogates of mineral dust. Atmos. Chem. Phys. 7, 5081–5091.
Mikhailov, E.F., Vlasenko, S.S., Kiselev, A.A., Pyshkevich, T.N., 1998. Restructuring factors of soot particles. Atmos. Ocean Phys. 34, 307–317.
Mikhailov, E.F., Vlasenko, S.S., Kramer, L., Niessner, R., 2001. Interaction of soot aerosol particles with water droplets: influence of surface hydrophilicity. Aerosol Sci. 32, 697–711.
Moehler, O., Linke, C., Saathoff, H., Schnaiter, M., Wagner, R., Schurath, U., 2005. Ice nucleation on flame soot aerosol of different organic carbon content. Meteorol. Z. 14, 477–484.
Muller, E.A., Rull, L.F., Vega, L.F., Gubbins, K.E., 1996. Adsorption of water on active carbons: a molecular simulation study. J. Phys. Chem. 100, 1189–1196.
Ohta, S., Okita, T., 1984. Measurements of particulate carbon in urban and marine air in Japanese area. Atmos. Environ. 18, 2329–2423.
Onischuk, A.A., diStasio, S., Karasev, V.V., Strunin, V.P., Baklanov, A.M., Panfilov, A.V., 2000. Evidence for long-range coulomb effects formation of nanoparticles agglomerates from pyrolysis and combustion routes. J. Phys. Chem. 104, 10426–10434.
Petzold, A., Strom, J., Ohlsson, S., Schröder, F., 1998. Elemental composition and morphology of ice-crystal residual particles in cirrus clouds and contrails. Atmos. Res. 49, 21–34.
Persiantseva, N.M., Popovicheva, O.B., Shonija, N.K., 2004. Wetting and hydration of insoluble soot particles in the upper troposphere. J. Environ. Monit. 6, 939–945.
Pitter, R.L., Pruppacher, H.R., 1973. A wind tunnel investigation of freezing of small water droplets falling at terminal velocity in air. Q. J. R. Meteorol. Soc. 99, 540–550.
Popovicheva, O.B., Persiantseva, N.M., Rulev, G.B., Shonija, N.K., Buriko, Y.Y., Starik, A.M., Demirdjian, B., Ferry, D., Suzanne, J., 2000. Experimental characterization of aircraft combustor soot: microstructure, surface area, porosity and water adsorption. PCCP 2, 4421–4426.
Popovicheva, O.B., Persiantseva, N.M., Kuznetsov, B.V., Rakhmanova, T.A., Shonija, N.K., Suzanne, J., Ferry, D., 2003a. Microstructure and water adsorbability of aircraft combustor soots and kerosene flame soots: toward an aircraft-generated soot laboratory surrogate. J. Phys. Chem. A 107, 10046–10054.
Popovicheva, O.B., Persiantseva, N.M., Shonia, N.K., Zubareva, N.A., Starik, A.M., Secundov, A.N., Usenko, D.A., Zakharov, V.M., Suzanne, J., Ferry, D., Demirdjian, B., 2003b. Aircraft engine soot: characteristic properties as CCN in upper troposphere. In: Roy, G.D., Frolov, S.M., Starik, A.M. (Eds.), Combustion and Atmospheric Pollution. Torus Press, Moscow, pp. 444–449.
Popovicheva, O.B., Persiantseva, N.M., Lukhovitskaya, E.E., Shonija, N.K., Zubareva, N.A., Demirdjian, B., Ferry, D., Suzanne, J., 2004. Aircraft engine soot as contrail nuclei. Geophys. Res. Lett. 31 Art. No. L11104.
Pruppacher, H.R., Klett, J.D., 1978. Microphysics of Clouds and Precipitation. Reidel, Dordrecht. ch.9.
Riemer, N., Vogel, H., Vogel, B., 2004. Soot aging time scales in polluted regions during day and night. Atmos. Chem. Phys. 4, 1885–1893.
Rogers, D.C., DeMott, P.J., Kreidenweis, S.M., 2001. Airborne measurements of tropospheric ice nucleating aerosol particles in the Arctic Spring. J. Geophys. Res. 106, 15053–15063.
Schrader, M.E., 1975. Ultra vacuum techniques in the measurement of contact angles. IV. Water on graphite (0001). J. Phys. Chem. 79, 2508–2515.
Seeley, L.H., Seidler, G.T., 2001. Preactivation in the nucleation of ice by Langmuir films of aliphatic alcohols. J. Chem. Phys. 114, 110464–110470.
Shonija, N.K., Popovicheva, O.B., Persiantseva, N.M., Savel'ev, A.M., Starik, A.M., 2007. Hydration of aircraft engine soot particles under plume conditions: effect of sulfuric and nitric processing. J. Geophys. Res. 112, D02208. doi:10.1029/1006JD007217.
Stockel, P., Weidinger, I.M., Baumgartel, H., Leisner, T., 2005. Rates of homogeneous ice nucleation in levitated H_2O and D_2O droplets. J. Phys. Chem. A. 109, 2540–2546.
Strom, J., Ohlsson, S., 1998. In situ measurements of enhanced crystal number densities in cirrus clouds caused by aircraft exhaust. J. Geophys. Res. 103, 11355–11361.
Twohy, C.H., Poellot, M.R., 2005. Chemical characteristics of ice residual nuclei in anvil cirrus clouds: evidence for homogeneous and heterogeneous ice formation. Atmos. Chem. Phys. 5, 2289–2297.
Vartapetyan, R.S., Voloshchuk, A.M., 1995. The mechanism of the adsorption of water molecules on carbon adsorbents. Russ. Chem. Rev. 64, 985–1001.
Zettlemoyer, A.C., McCafferty, E., 1973. Water on oxide surfaces. Croat. Chem. Acta 45, 173–186.
Zuberi, B., Betram, A., Cassa, C., Molina, L., Molina, M., 2002. Heterogeneous nucleation of ice in (NH4)2SO4–H2O particles with mineral dust immersions. Geohys. Res. Lett. 29, 1504. doi:10.1029/2001GL014289.